Integrating Microfluidics and Integrated Circuits toward a CMOS-Based Cell Counter

by
Kevin Bishop

A THESIS

submitted to

Oregon State University

Honors College

in partial fulfillment of
the requirements for the
degree of

Honors Baccalaureate of Science in Electrical & Computer Engineering
(Honors Scholar)

Presented June 4, 2018
Commencement June 2018

AN ABSTRACT OF THE THESIS OF

Kevin Bishop for the degree of Honors Baccalaureate of Science in Electrical & Computer Engineering presented on June 4, 2018. Title: Integrating Microfluidics and Integrated Circuits toward a CMOS-Based Cell Counter.

Abstract approved:_____

Matthew L. Johnston

Cell counting is a key tool used in biological and clinical laboratories, but at present, commercial cell counters are large and expensive. CMOS technology is a promising platform for creating small, low-cost sensors but currently lacks a robust method of directly interfacing these sensors with the microfluidic networks needed for sample delivery. We present two methods of microfluidic integration. The first is a laser-cut fabrication method for rapid prototyping of devices; it uses only standard 'maker' tools and a completed device can be fabricated in under one hour. The second, higher resolution, method uses photolithography to define SU-8 channels that can be created on the scale of single cells. A method of planar, metallized electrical connections to the IC is also described that can implemented with either fluidic method above. A completed device shows that leak-free channels can route fluid directly over a SPAD light sensor with metal connections, representing an important milestone toward a fully-integrated CMOS-based cell counter.

Key Words: cell counting, CMOS sensors, microfluidics

Corresponding e-mail address: kevinwarnerbishop@gmail.com

Integrating Microfluidics and Integrated Circuits toward a CMOS-Based Cell Counter

by
Kevin Bishop

A THESIS

submitted to

Oregon State University

Honors College

in partial fulfillment of
the requirements for the
degree of

Honors Baccalaureate of Science in Electrical & Computer Engineering
(Honors Scholar)

Presented June 4, 2018
Commencement June 2018

Honors Baccalaureate of Science in Electrical & Computer Engineering project of Kevin Bishop presented on June 4, 2018.

APPROVED:

_____

Matthew L. Johnston, Mentor, representing Electrical & Computer Engineering

_____

Li-Jing Cheng, Committee Member, representing Electrical & Computer Engineering

_____

Shaan Sengupta, Committee Member, representing Electrical & Computer Engineering

_____

Toni Doolen, Dean, Oregon State University Honors College

I understand that my project will become part of the permanent collection of Oregon State University, Honors College. My signature below authorizes release of my project to any reader upon request.

_____

Kevin Bishop, Author

Acknowledgements

I would like to thank Dr. Matthew Johnston for his invaluable mentorship both on this project and throughout my time at Oregon State University. His support and guidance helped lead me to the decision to pursue a career in academic research. Thank you also to Dr. Larry Cheng and Shaan Sengupta for their willingness to serve on my thesis committee.

Additionally, I would like to thank Megan Co for her partnership in developing the laser-cut microfluidics platform, and SIM Lab members Kyle Clocker, Jacob Dawes, and Hyunkyu Ouh for technical guidance throughout this project.

Finally, thank you to the Oregon State University Honors College for providing financial support for this project through a DeLoach Work Scholarship.

1. Introduction

A number of processes in both scientific and clinical laboratories require counting and characterization of cells suspended in fluid. This is relatively easy to accomplish with existing benchtop instruments, however a cheap, fully-portable cell counting platform that can compete with these instruments remains an elusive goal of researchers and engineers. Our lab, the Oregon State University Sensors and Integrated Microelectronics Laboratory (SIM Lab) has previously done work investigating ways to interface complementary metal-oxide-semiconductor integrated circuit (CMOS IC)-based sensors with microfluidic sample delivery. We hope to ultimately create a CMOS-based cell counter as a key demonstration of our platform.

This work represents a major step towards a CMOS-based cell counter. Previously, our lab demonstrated a single-photon avalanche diode (SPAD) ambient light sensor created on a CMOS IC [1] as well as a method of packaging ICs in epoxy coupons for planar feature integration. For this work, a method of creating microfluidic channels was created that allows fluid samples to be delivered to a SPAD ambient light sensor (we briefly discuss a portion of this process, as well as the method of epoxy packaging, in [2]; this work describes the fluidic integration process in greater detail). The device was tested via inspection under a microscope to check for leaks in the channel and effective fluidic integration. Future steps to extend the work described here will be to characterize the sensor output of the device using a dye solution and polymer beads, followed by testing with real cells. Future research will also explore fluorescent labeling options that would allow differentiation between different types of cells.

2. Cell Counting Overview and Applications

At its core, cell counting determines the concentration and properties of cells present in a sample, generally independent cells suspended in a fluid matrix. Cell counting has a number of applications in biology and medicine, both at the basic science and clinical levels. One example is a CD4 count, which determines the concentration of T helper cells (also known as CD4 cells) present in a person's blood. T Helper Cells are responsible for instigating or suppressing the response of other immune cells, playing a critical role in the body's immune system. HIV weakens the immune system by attacking T Helper Cells, making a person more vulnerable to infection. As such, a CD4 count is used as a primary measure of HIV progression and treatment success. CD4 counts also provide a helpful general metric of a person's immune health.

Another application is a complete blood count, which determines the concentration of white blood cells, red blood cells, platelets, and hemoglobin in the blood. More sophisticated cell counters can further differentiate between different types of cells in each of these broad categories, providing additional information to physicians. An increased monocyte (a type of white blood cell) count, for example, can accompany malaria or tuberculosis, while an increased eosinophil count (another type of white blood cell) occurs in parasitic infections. A physician can use this information as a diagnostic aid to determine the best course of treatment for a patient.

Complete blood counts also find a number of applications in cancer diagnosis and treatment. The blood counts of people with cancer, in particular those undergoing chemotherapy, fluctuate rapidly and must be monitored regularly to ensure treatment

is going as intended. Cancer treatment would benefit from technology enabling regular blood counts from home in addition to those already done in a clinical setting. For example, a fever can be a life-threatening condition for a person undergoing chemotherapy if their white blood cell (WBC) count is low, however it is not especially problematic if this count is normal. As such, people undergoing chemotherapy who develop a fever are generally sent to the emergency room immediately. A reliable home blood count would avoid unnecessary emergency room visits and the associated risk and cost by allowing patients with normal WBC counts to stay home. Another example is treatment of certain cancers via bone marrow transplant. Patients can stay in the hospital for around three weeks following a transplant, and some of these patients are there exclusively for close blood count monitoring. A home blood count device would allow these people to recover at home, again avoiding the additional risks and costs associated with lengthy hospital stays [3].

The device presented here was created with the application and scale of cell counting in mind, however it could be more broadly applied to measuring the concentration of any type of particle suspended in fluid. Particle counters in general have a variety of uses beyond the aforementioned biomedical applications. The concentration of solid particles present in water could be a measure of its potability. Likewise, an excessive concentration of dissolved particles in a drug for injection or in hydraulic fluid could indicate the substance is contaminated and not suitable for use.

2.1 Specific Methods of Cell Counting

Most methods of cell counting share two main elements: a focusing stage and a detection stage (Fig. 1). In the focusing stage, the sample is confined to a narrow detection area such that a relatively small number of cells are passing through the detection region at a given time. In the second stage, a sensor is placed at the detection region such that each time a cell passes the detector, it is counted. The concentration of cells can then be computed using the number of cells detected in a given period of time and the rate at which the sample is flowing. Advanced devices may categorize detected cells based on size or other characteristics.

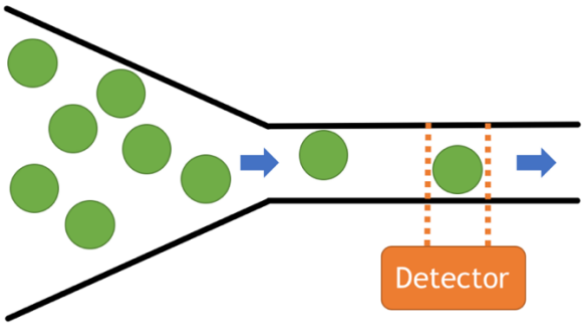

Fig. 1 General schematic of a cell counter. Cells are lined up single-file in the focusing stage (left) and then counted as they pass through a detector one at a time (right).

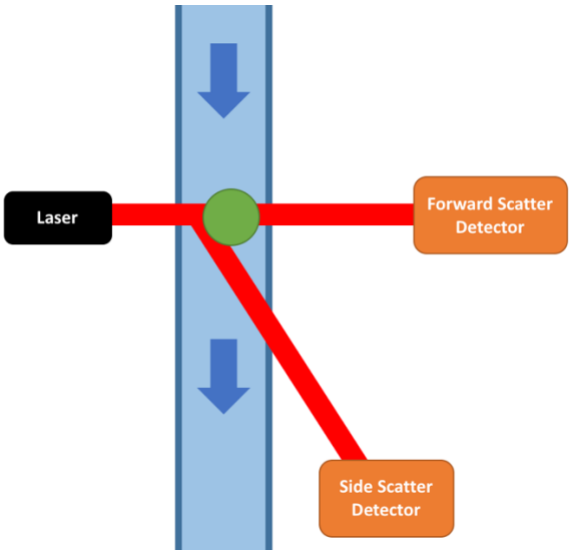

Fig. 2 Optical schematic of a flow cytometer.

Flow cytometry is the current state-of-the-art method of cell counting. In flow cytometry, cells are focused into a single file stream of cells in fluid and are passed, one by one, through a laser beam (Fig. 2). Light from the laser is scattered when it hits each cell and is detected by light sensors positioned around the detection region. The degree and direction of scattering is analyzed to give information on the cell's size and shape, yielding information on the type of cell being detected. Cells can also be fluorescently labeled (see section below), allowing further classification by cell type. Flow cytometry boasts high accuracy and throughput at the cost of being relatively complicated to implement. The technique requires fine laser alignment, complex optics, and robust analytical software; systems are large and expensive, making them impractical for low volume or resource limited settings.

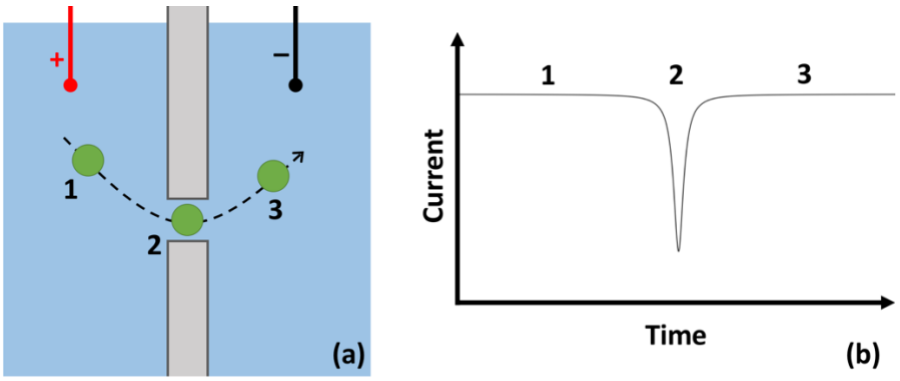

Fig. 3 (a) Schematic of a Coulter counter showing a cell passing through an aperture connecting two electrolyte reservoirs. (b) Plot of current between the two sides showing a drop as the cell passes through the aperture.

An alternative to flow cytometry is the implementation of a Coulter counter. A Coulter counter consists of two reservoirs of electrolyte solution that are connected by a small (approaching cell-sized) aperture (Fig. 3). Each chamber contains an electrode such that current flows between them through the aperture. The cells to be counted start in one reservoir and are pumped through the connection to the other. Each time a cell passes through the aperture, it displaces some of the solution in the connection and results in a change in the impedance between the two chambers. This change is detected by the measuring the current through and voltage across the electrodes, and the degree of the change provides information about the size or resistivity of the cell.

2.2 Fluorescent Labeling

Labeling refers to the process of tagging substances that are difficult to detect on their own with an easier to detect substance, or label. A label is a molecule that only attaches to a specific type of particle or cell. Often, labels are fluorescent, meaning they give off a signature wavelength of light when excited with another wavelength of light.

As a result, one can distinguish between different types of cells based on the signature wavelength of light emitted by their labels. For example, two labels could be added to an unknown population of cells: a red label for cat blood cells and a green label for dog blood cells (Fig. 4). A cell is selected and hit with an excitation wavelength. If it emits red light, it is a cat blood cell; if it emits green light, it is a dog blood cell.

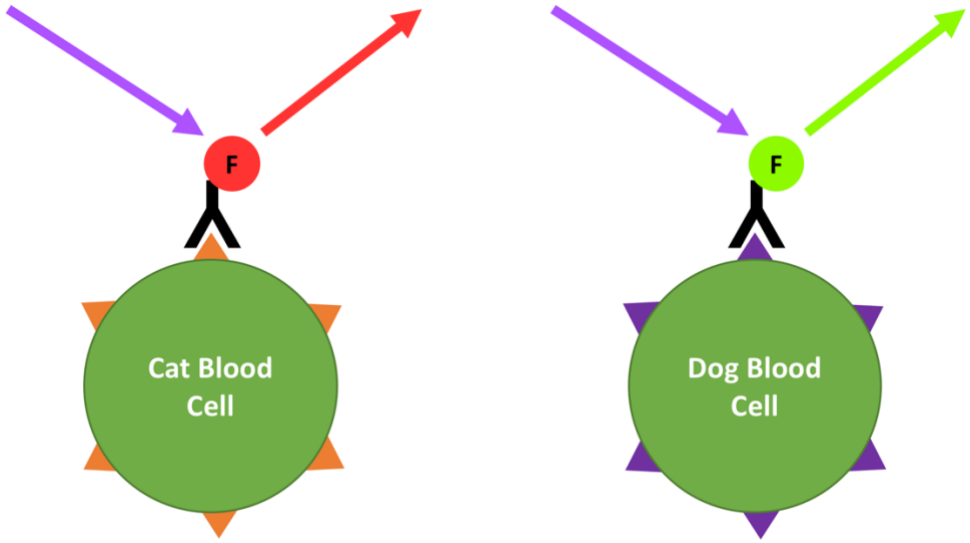

Fig. 4 Diagram showing fluorescent cell labeling. The cat blood cell has surface antigens that are recognized exclusively by red fluorescent labels, while the dog blood cell has surface antigens that are only recognized by green fluorescent labels.

3. CMOS Cell Counters

Complementary metal-oxide-semiconductor (CMOS) integrated circuits (ICs) are electronic circuits that, instead of being made of discrete components, are manufactured on a single piece of silicon. This allows ICs to be smaller and faster than their discrete counterparts, with thousands or millions of components possible in a coin sized device. In the context of a sensing platform, sensors (light sensitive photodiodes,

for example) are typically built onto the surface of the IC for direct interfacing with both the sample and the associated electronics.

CMOS ICs paved the way for rapid advances in computing as well as analog signal processing over the past half-century. More recently, this progress has been translated to biomedical applications to spur advances in biosensing using the techniques developed for CMOS ICs or, in many cases, making use of ICs directly. For example, an on-chip DNA detection system for hepatitis B virus has been demonstrated [4]. In this system, a cantilever-based method of DNA detection is fully-integrated with sensing circuitry on a CMOS chip. The method is label-free and requires minimal sample preparation, making it a prime example of an integrated CMOS-based biosensor. Other examples of CMOS-based biosensors include an impedance-based molecular biosensor that uses changes in impedance to detect particular proteins or DNA strands [5] (Fig. 5) and an integrated, massively parallel device for DNA sequencing that leverages CMOS technology to integrate 1.2 million sensing sites on a single chip [6].

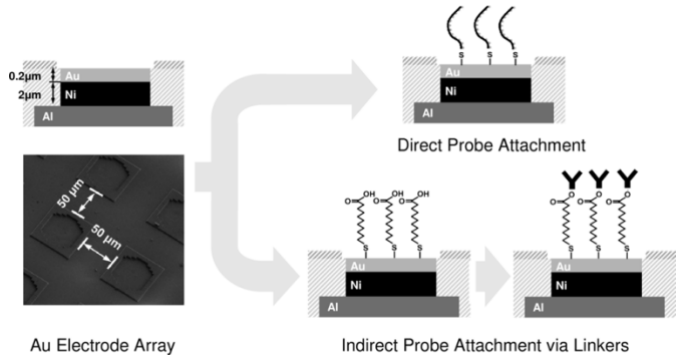

Fig. 5 Cross-section of CMOS sensor platform based on impedance changes resulting from biomolecule adhesion to substrate. SEM image of the device surface is also shown. This is an example of a CMOS-based biosensor. Originally from [5].

3.1 Fluidic Integration

In CMOS cell counters, the same two key problems exist that are present in conventional cell counters: delivering the sample to the sensor and detecting the cells in the sample. In the case of an integrated CMOS cell counter, the task of sample delivery typically takes the form of microfluidic integration on the IC. Microfluidic devices are systems that manipulate fluids on the scale of micro- or nanoliters. The emergence of microfluidics has allowed laboratories to achieve both higher throughput and lower sample consumption than is possible with macro-scale methods. Conventional microfluidic devices employ polydimethylsiloxane-casted (PDMS, a semi-flexible polymer) channels for fluid manipulation [7]. In this method, channels are cast in PDMS from a photolithographically-defined master mold.

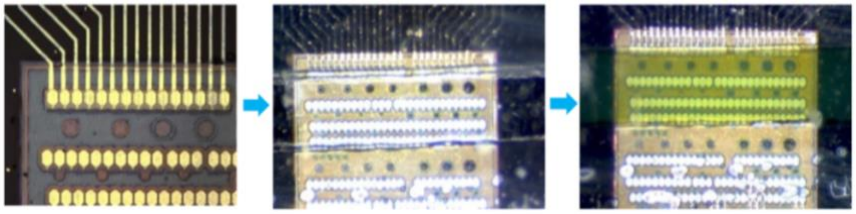

Fig. 6 Our past method of fan-out wafer-level packaging to create planar metal connections to an epoxy-molded IC, allowing direct addition of planar microfluidics. Bare connections, unfilled, and filled fluid channels are shown. Originally from[2].

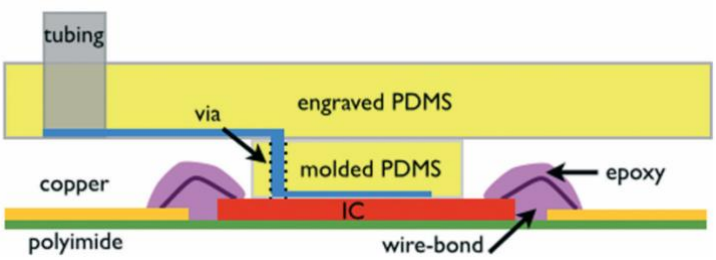

Fig. 7 Cross sectional view of stacked PDMS interfacing method, allowing wire-bonds and PDMS fluid channels to exist on the same chip. Originally from [8].

CMOS-chips, however, require more complex techniques to allow electrical connections to the CMOS chip and fluidic connections to the surface sensor to exist without interfering with one another. Both the input (fluidics) and output (electrical connections) of the sensor must connect externally in order for the sensor to function. Several methods have been presented to achieve this, including modifications to the basic PDMS scheme or new techniques altogether. We have previously presented a method for interfacing fluidic networks with CMOS-based sensors [7]. This method uses a fan-out wafer-level packaging technique to allow for fluidic access to the entire surface of the device without obstruction by wire bonds to the IC (Fig. 6). Other groups have presented alternative approaches to this problem. One demonstrates a PDMS-based fluidic network that is elevated above electrical connections using a small, molded PDMS block through which fluidic channels pass [8] (Fig. 7). Another approach replaces wire-bonded electrical connections with soldered and photolithographically defined connections; a PDMS-based fluidic layer is then placed directly over the IC [9]. While these techniques successfully bridge the interface between fluidics and sensors, no method to date allows channels to be created directly

as part of the CMOS fabrication process. Such a method would allow fully-integrated fabrication of a sensor, lowering device size and cost.

3.2 Signal Transduction

The second main challenge to producing a CMOS-based microfluidic cell counter is that of actually detecting cells when they are delivered to the detection region. The most promising methods for doing so can be broadly categorized as either optical detection or electrical detection. In optical detection, cells change the amount of light reaching a sensor as they pass by it (Fig. 8), either by casting a shadow to block ambient light or emitting additional light via fluorescent labeling; this is the micro-scale analog to the macro-scale method of flow cytometry described above. In electrical detection, cells pass between two electrodes and disrupt the current path between them, changing either the magnitude (DC) or frequency (AC) of the signal; this is akin to the Coulter counting method described above.

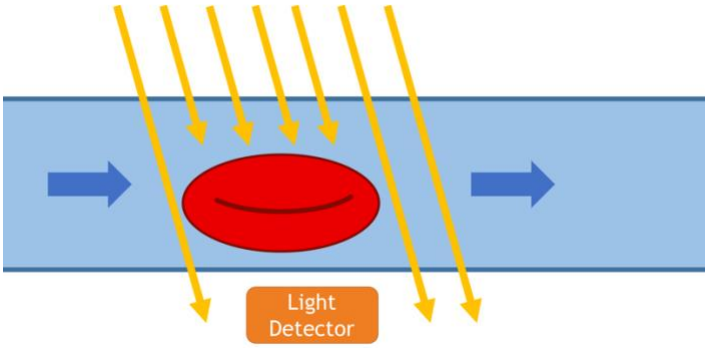

Fig. 8 Principle behind optical cell counting schemes. Cells cast shadows as they pass one at a time through a microfluidic channel over a light sensor.

A number of novel optical methods have been presented, for example using a charge coupled device (CCD) camera to aggregately detect fluorescently labeled cells [10]. In addition, the field of CMOS-based optical sensing in a broader sense has been well explored, resulting in, for example, CMOS ambient light sensors [11]. Several groups have also demonstrated electrical-impedance-based methods of cell counting using microfluidic channels [12], [13].

3.3 Existing CMOS Cell Counters

Creating a fully-integrated CMOS cell counter requires solutions to both of these challenges: successfully interfacing microfluidic channels with CMOS circuits to deliver a sample to a sensing region and optically or electrically detecting the sample once it is delivered. In one of the most mature optical CMOS cell counting schemes to date, a system is developed to count fluorescently labeled cells based on identity and size [14]. A CMOS SPAD array sensor is used to detect labeled particles and beads, and fluidic integration is completed using a PDMS cartridge placed over the array. Rather than passing cells over individual sensors, the device uses an aggregate approach to run cells over the entire array and then averages the result. The SPAD setup also results in a pseudo-digital cell count, simplifying processing software and hardware.

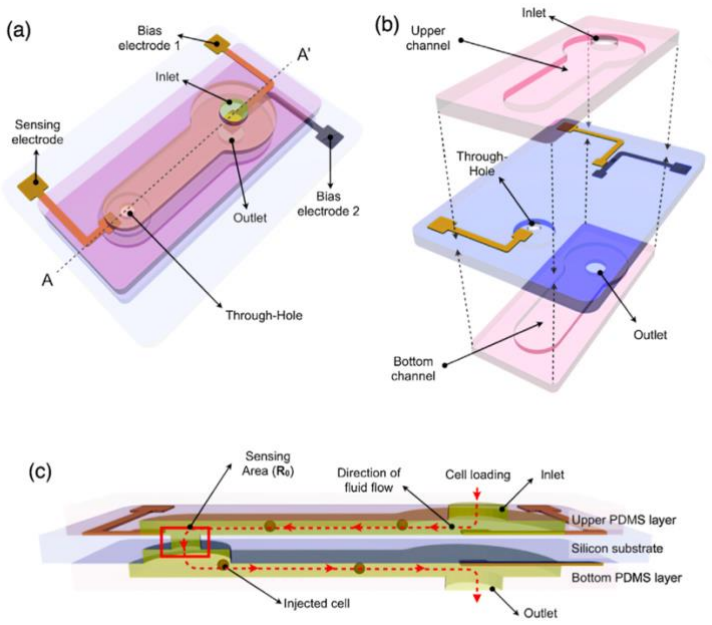

Fig. 9 Schematic of a two-layer Coulter counter detection device showing (a) top view, (b) expanded view, and (c) side view with cell in transit. Originally from [15].

A sophisticated electrical cell counter has also been demonstrated [15]. While not, strictly speaking, CMOS-based, this device is a single chip, fully-integrated Coulter counter manufactured on a wafer with microfluidic integration. The device consists of a two-layer channel in which cells pass through a via between the layers (Fig. 9). As in the previous system, PDMS is used to fabricate the channel layers. In the via, sensing occurs as cells disrupt an electrical current traveling between the two layers (provided by a bias electrode in each layer). The events are detected using changes in the voltage drop across the via. The system can reliably distinguish between different sized microbeads on the order of microns and is also shown to be able to detect the concentration of cancer cells in a diluted blood sample.

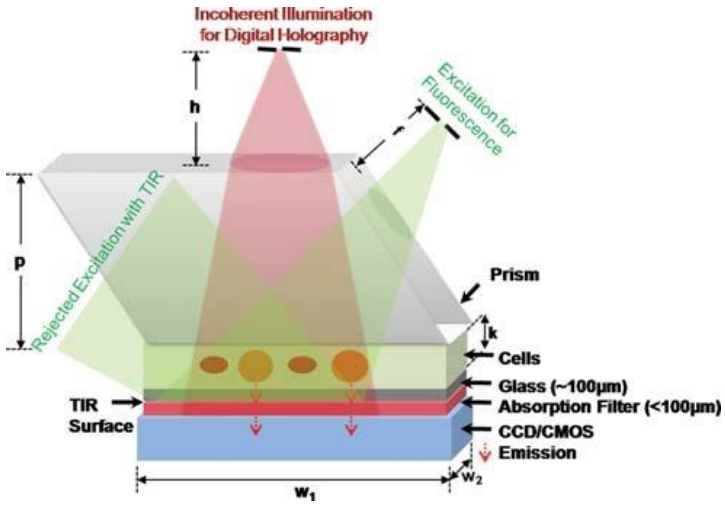

Fig. 10 Optical schematic of aggregate cell counter based on CCD or CMOS array. Originally from [16].

Finally, a partially integrated, CMOS-based cell counter has been shown [16]. This device is notable for its departure from the approach of running cells past a detector one at a time. Instead, the device consists of an on-chip imaging chamber placed directly over a large CCD or CMOS array (Fig. 10). An image of the entire chamber is captured and processed to extract a cell count; this data is then deconstructed into information about individual cell concentrations. Though this solution is not fully-integrated in CMOS, it provides a relatively compact method of high-throughput cell counting using an unconventional aggregate counting approach as an alternative to single cell microfluidic channels.

4. Methods and Results

As discussed previously, there are two primary technical challenges to making a microfluidic cell counter: delivering cells one at a time to the sensor and detecting cells as they pass. Here, a single-photon avalanche diode (SPAD) light detector

embedded in the surface of an IC is used to create an optical detection platform. This IC is embedded in epoxy to create a continuous substrate on which microfluidic delivery networks can be built. Two novel alternatives to PDMS-based fluidic networks were explored. The first is a laser-cut method of channel definition intended for rapid and low-cost prototyping, and the second is a photolithographic, SU-8-based approach for higher definition applications. The SU-8 approach was used in the final device.

4.1 SPAD Optical Detection and Epoxy Molding

To detect individual cells, an optical detection scheme previously developed by our lab [16] is implemented. A SPAD ambient light sensor sits on the floor of the fluidic channel (formed by the surface of an IC) and is used to detect shadows cast as cells pass over it. The SPAD works by holding a silicon PN junction beyond its breakdown voltage. This creates a volatile state in which a single photon incident on the junction causes an influx of forward current that can be interpreted as a digital pulse. The advantage of this scheme is that the pseudo-digital output of the SPAD can be fed directly into a comparator and then to a microcontroller, eliminating the need for analog-to-digital conversion circuitry. As the junction is sensitive to single photons, a layered-metal optical filter was included in the CMOS design on the device's surface to prevent saturation in ambient light conditions.

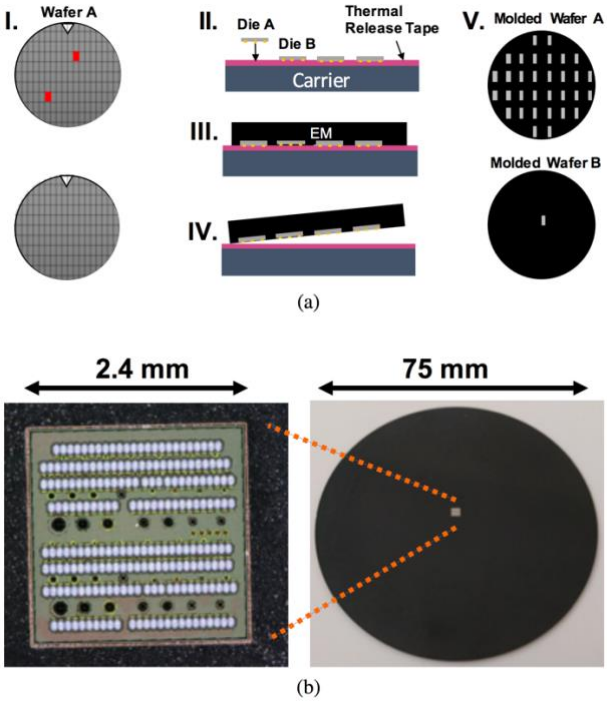

Fig. 11 (a) Process flow diagram of epoxy molding process. A wafer is diced (I) and each die is placed face down on a carrier substrate covered in thermal release tape (II). The dice are covered in epoxy (III) which is then cured, allowing the assembly to be lifted off (IV) leaving an IC embedded in an epoxy coupon (V). (b) Image of an example coupon embedded with an IC. Originally from [17].

In order for microfluidic channels to seal fully to the surface of an IC, a flat, continuous face needs to be created on which channels are built. To provide such a surface, ICs previously molded in an epoxy coupon using a process described in [17] are used (Fig. 11). In this technique, the fabricated IC is placed face down on a carrier substrate. The IC is then covered and compression molded in semiconductor-grade epoxy mold compound (EMC). Once released and cured, the resulting epoxy coupon forms a continuous substrate flush with the surface of the IC.

4.2 Metallized Electrical Connections

To control the SPAD and receive the output data, electrical connections must be made to metal pads on the IC's surface. The challenge here lies in creating connections that do not interfere with the fluidic channels needed to deliver cells to the sensor. The conventional method of connecting to ICs is wire bonding, a process in which physical metal wires arc to the pads on the IC and extend out to connect to a microcontroller or other processor. The wires would create a nonplanar surface on the coupon, rendering simple microfluidic integration impossible. To overcome this obstacle, wire bonds have been replaced here with photolithographically-defined, thin-film metal connections on the surface of the coupon. These connections extend the IC pads outwards beyond the area needed for fluid channels to pads that can then be connected electrically.

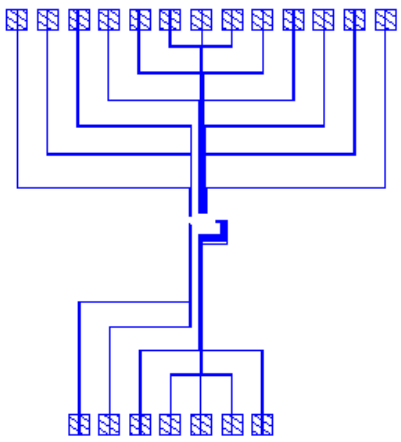

Fig. 12 Mask design used for metallization process. Blue regions are openings in the mask and match the aluminum pattern.

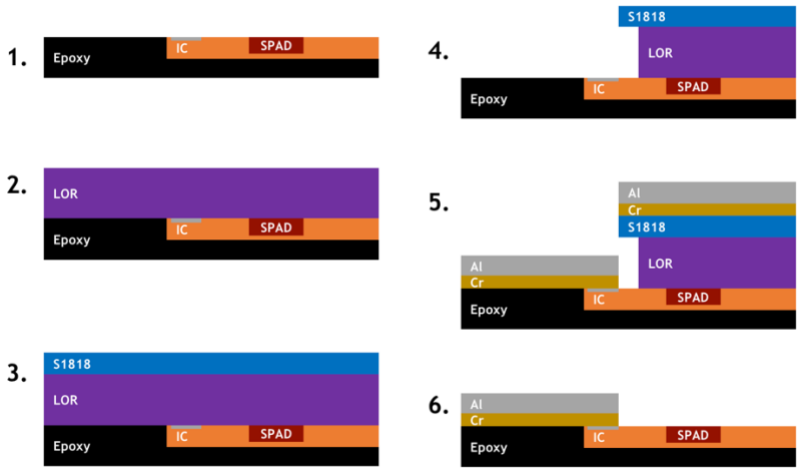

Fig. 13 Process flow diagram of metallization process (the thickness of aluminum and chrome is exaggerated here; it is negligible in reality). Beginning with an epoxy-molded IC, LOR and S1818 photoresist are spun on. Photoresist is exposed and dissolved in areas where connections are needed. Aluminum (with chrome adhesion layer) are deposited and photoresist is dissolved, leaving metal connections.

To create the metal layer, a chrome mask (Fig. 12) is created with openings where metal is to be deposited. Liftoff resist 30B (LOR, MicroChem, Westborough, MA) followed by S1818 (MicroChem, Westborough, MA) are then applied to the surface of the coupon and exposed through the created mask to UV light (Fig. 13). S1818 is a positive photoresist, meaning that the region exposed can be subsequently dissolved during the development step (MF-321 developer, MicroChem, Westborough, MA), while the unexposed regions remain solid. A thin aluminum layer is then applied to the coupon's surface via thermal evaporation. As aluminum does not adhere well to the epoxy substrate on its own, a thin chrome adhesion layer is applied first. Finally, the remaining photoresist is dissolved (Remover PG, MicroChem, Westborough, MA), removing the metal on top of the resist and leaving the desired metal pattern on the surface of the coupon.

Aluminum was the selected metal here as it is relatively inexpensive and our methods and infrastructure to metallize epoxy coupons in aluminum are well developed. It is of note, however, that aluminum is not an ideal material in some situations (chiefly in that it is difficult to solder to directly). In some applications, other metals (copper, for example) may be more appropriate. Based on the work done for this project, there is no reason to believe the results could not be replicated in another metal as needed.

The LOR is used to create a cleaner metal pattern than is possible with S1818 alone. LOR is not photosensitive and can be dissolved by the S1818 developer. After the exposed S1818 region is dissolved, the developer begins to dissolve the LOR laterally, creating an undercut as opposed to a continuous sheer face as is the case with S1818 alone (Step 4 in Fig. 13). If LOR is absent, the metal tends to create a continuous layer across the sheer face. When the photoresist is dissolved in this case, the unwanted metal can pull off regions of the desired pattern with it, causing rough edges and gaps in the connections. An undercut prevents metal from adhering to the vertical surface of the photoresist, ensuring the unwanted metal region is physically separate from the desired region and can be cleanly removed.

Beginning with an epoxy molded IC, the metallization process is as follows:

1. Clean substrate with acetone followed by isopropyl alcohol; blow dry and bake for 2 minutes to fully dehydrate.

2. Add LOR to cover roughly 80% of the surface. Spin at 500 rpm with 500 rpm/s ramp for 10 seconds to spread and follow immediately by spinning at 4000 rpm with 1000 rpm/s ramp for 40 seconds to thin.
3. Soft bake on a hotplate at 170˚C for 10 minutes and cool for at least 2 minutes.
4. Add photoresist to cover roughly 70% of the surface. Immediately spin at 3000 rpm with 5000 rpm/s ramp (or maximum ramp) for 30 seconds.
5. Bake on a hotplate at 115˚C for 90 seconds and blow to cool.
6. Alight the substrate under the mask and expose to UV light (350W Hg lamp) for 10 seconds.
7. Develop in MF-321 for 2 minutes, agitating continuously. Immediately place in water bath, rinse with additional DI water, and blow dry.
8. Examine substrate under microscope to check for a visible undercut and repeat development 1 minute at a time until undercut appears. Three minutes of total development time was sufficient for this work.
9. Remove excess material using an O_2 plasma ash for 1 minute at 50W.
10. Deposit chrome via thermal evaporation over surface to a thickness of 20 nm.
11. Deposit aluminum via thermal evaporation over surface to a thickness of 150 nm; vacuum should not be broken between this and the previous step.
12. To lift off excess metal, submerge substrate in Remover PG and leave, covered, for 1 hour. Rinse with isopropyl alcohol.
13. Dislodge metal via ultrasonic bath for 1-2 minutes and rinse again with isopropyl alcohol.

14. Repeat Remover PG/ultrasonic bath process until excess metal is fully removed. *Throughout the lift off stage, the substrate should be either submerged or continuously bathed so that it does not dry. Drying can cause stray aluminum to adhere permanently to the surface.*

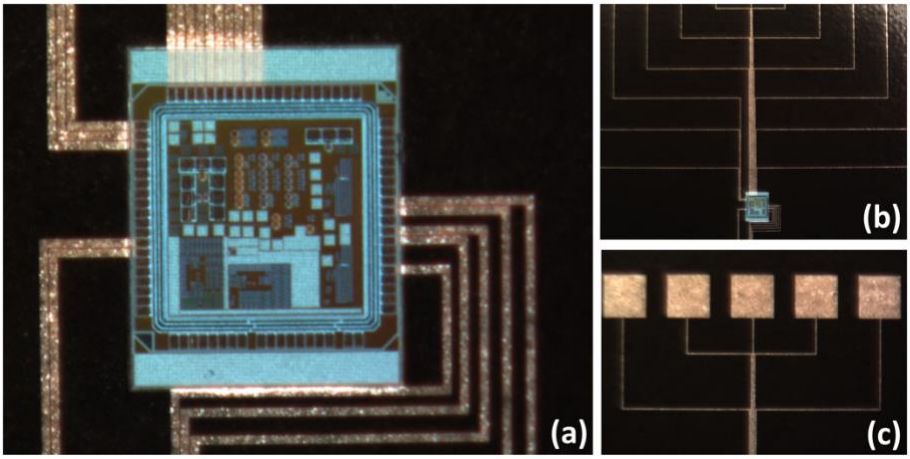

Fig. 14 Epoxy-molded IC after metallization showing (a) closeup of connections to IC, (b) connections routing up away from IC, and (c) connection pads.

Fig. 14 shows closeups of an epoxy-molded IC after metallization. After the coupon has been metalized, one of the two microfluidic channel fabrication methods described below is used to route a cell-containing fluid sample over the SPAD.

4.3 Laser-Cut Fluidic Channels

The laser-cut microfluidics process first developed allows channels to be created using standard 'maker' tools in a matter of minutes compared to hours or days needed to create PDMS or SU-8 devices. Laser-cut devices consist of a 9474LE 300LSE pressure sensitive adhesive (PSA) sheet (3M, Maplewood, MN) sandwiched between two pieces of acrylic (Fig. 15). A channel pattern is designed using CAD

software (Inkscape was used for this work) and cut out of a PSA sheet using a consumer benchtop laser cutter. Fig. 16 shows several example channel patterns. Two pieces of acrylic are similarly designed and cut using the laser cutter, one solid piece that serves as the bottom of the device and another piece with holes cut at fluid inlets and outlets that serves as the device's top. Glass can also be used in place of acrylic to form the top and bottom layers; in this case holes are drilled using a diamond drill bit as opposed to laser cut. Acrylic was preferred here as laser cut holes can be created more quickly and placed more accurately. Glass substrates are also prone to breaking if drilled too quickly.

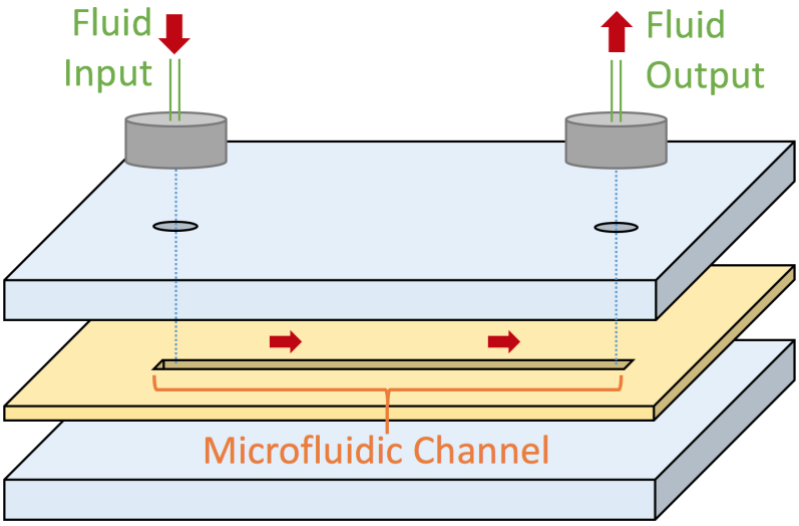

Fig. 15 Expanded view of laser cut microfluidic device. A laser-cut PSA sheet (yellow) is sandwiched between a top substrate with holes and a solid bottom substrate (blue). The top substrate can be either drilled glass or laser-cut acrylic, while the bottom substrate can be glass, acrylic, or (in the case of this work) an epoxy coupon. Tubing adaptors on top allow for interfacing with external fluidic networks.

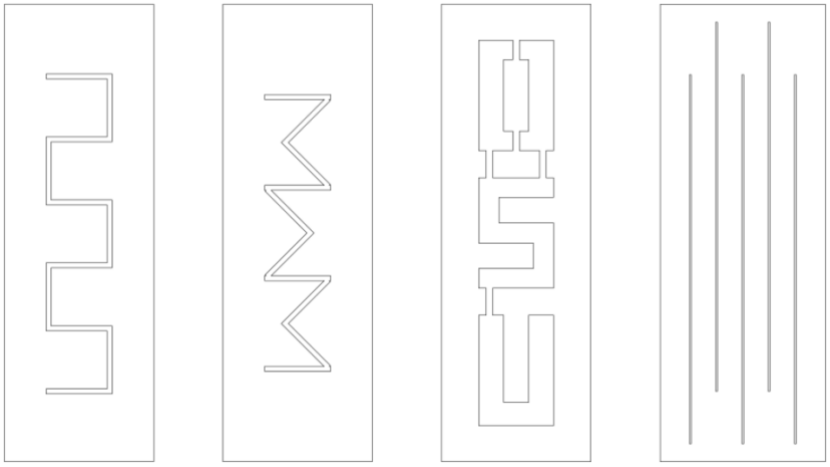

Fig. 16 Example laser-cut channel patterns showing that channels can be created with arbitrary complexity to angle, split, or change width as desired.

To interface with external fluidic elements, such as syringes or waste reservoirs, a press fit tubing connector is applied to the device's surface (Grace Bio-Labs, Bend, OR). These connectors consist of a flexible, doughnut-shaped block with adhesive on one side. A piece of tubing or luer stub tip can be inserted into the center, forming a fluid-tight seal to the channel. Open fluid reservoirs can similarly be created by cutting a larger hole in the acrylic layer. To apply this method to an IC-based sensor, the lower substrate is simply replaced with an epoxy-molded IC such that fluid runs directly over the sensor's surface.

Devices created using this method were examined under a microscope for leaks. Fully-sealed devices of down to 250 µm channel width and 750 µm spacing between separate channels can be created. All devices have a nominal channel height of 170 µm; this dimension is defined by the thickness of the PSA used. A device can be fully designed and fabricated in under 1 hour using only standard 'maker' tools. As the design is directly laser cut, there is no additional overhead involved to change the channel pattern.

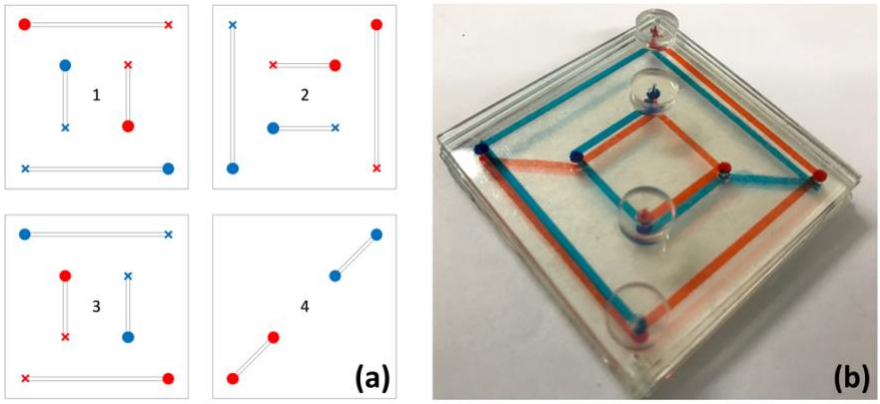

Fig. 17 An example of a multilayer fluidic device in which two separate channels (red and blue) circle each other in a double helix. (a) Dots in the schematic represent connections upwards, while crosses represent connections downwards. Layer 1 is the top layer while layer 4 is the bottom layer. (b) Assembled device with red and blue fluid running through channels.

This method can also be used to create three-dimensional fluid networks, which allow independent fluid channels to pass over one another. To accomplish this, additional PSA and acrylic layers are added, with laser-cut PSA defining higher-level fluid networks and acrylic layers forming fluidic vias between channel layers. An example of a helical 3D device is shown in Fig. 17. The design freedom used to create 3D devices similarly allows creation of devices of arbitrary size and complexity.

4.4 SU-8 Fluidic Channels

A more involved, higher-definition alternative to laser cutting fluidic channels is defining channels in SU-8. SU-8 is a negative epoxy photoresist. It is applied in a thin layer to a substrate and then specific regions are exposed to UV light, causing them to cure (Fig. 18). The uncured regions are dissolved away, leaving only the cured regions to define the channel. In this application, SU-8 2050 (MicroChem,

Westborough, MA) was used to create an approximately 50µm high and 100µm wide channel over the SPAD on the surface of the IC after metallization. The channel mask is show in Fig. 19. Next, a lid created from pressure sensitive adhesive (PSA) with a mylar coating was added to seal the channel. The lid includes tubing connectors at the input and output for interfacing with syringes for fluid delivery.

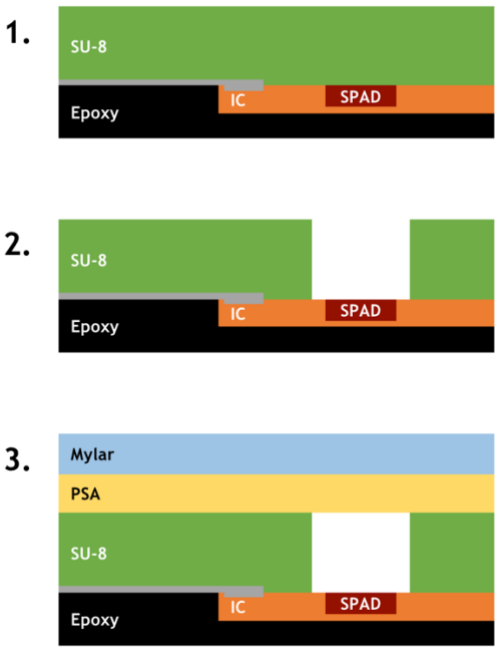

Fig. 18 Process flow diagram showing channel definition in SU-8 and addition of a PSA/mylar channel lid.

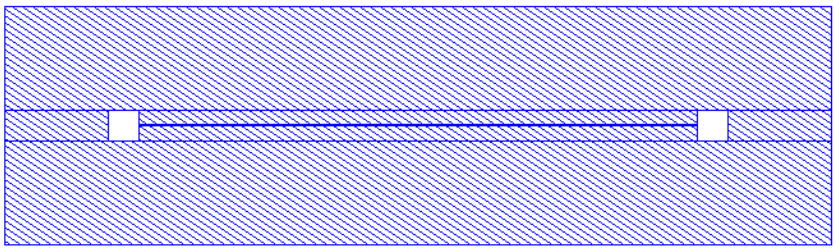

Fig. 19 Mask design used for SU-8 channel definition. Blue regions are openings in the mask and match the solid SU-8 pattern.

Beginning with a metallized, epoxy-molded IC, the process for defining channels is SU-8 is as follows:

1. Clean and prime the substrate using an O_2 plasma ash for 1 minute at 50W.
2. Add SU-8 to cover roughly 75% of the surface. Spin at 1000 rpm with 300 rpm/s ramp for 10 seconds to spread and follow immediately by spinning at 4000 rpm with 1000 rpm/s ramp for 30 seconds to thin.
3. Soft bake on a hotplate at 95˚C for 8 minutes.
4. Align the substrate under the mask and expose to UV light (350W Hg lamp) for 20 seconds.
5. Bake again at 95˚C for 5 minutes.
6. Develop in SU-8 developer for 2 minutes, agitating continuously. Immediately rinse with fresh developer followed by isopropyl alcohol; blow dry.
7. Remove excess material using an O_2 plasma ash for 1 minute at 50W.
8. Hard bake for 30 minutes at 165˚C.

After completing the process described above, we are left with a microfluidic trough in which the walls are formed by SU-8 and the bottom is formed by the surface of the IC/epoxy coupon. For proper microfluidic behavior, the channel also needs a lid. To be effective for use in an optical detection device, like the one described here, the lid must be optically transparent. It also must be sufficiently rigid and well-sealed to the channel walls to withstand the pressure of the fluid moving through the channel. The lid must serve as an interface between the microfluidic channel and a macro-scale fluid reservoir; leveraging the press fit tubing connectors described previously (Grace Bio-Labs, Bend, OR) is the obvious choice to accomplish this. Finally, the lid must be applied in such a way that it does not block the channel in the process.

Creating such a lid proved to be a challenging task. Our lab previously tried several methods of manually applying a lid to the channel. Manual application was promising as its success would enable simple, fully manual assembly of the lid without the need for a clean room or any special tools. However, the pressure needed to fully seal the channel, and particularly to apply the tubing connectors, causes the channel to collapse when applied manually.

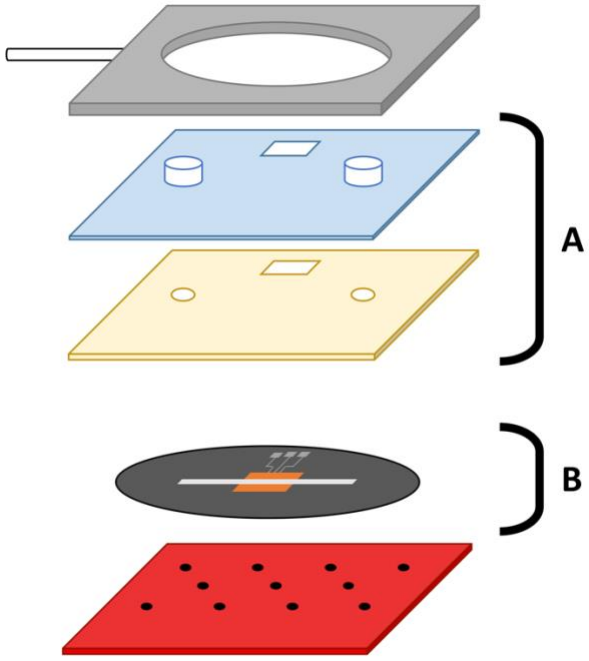

Fig. 20 Assembly diagram for channel lid. Mylar and PSA are sandwiched together. Holes for fluid channels and electrical connections to pads are laser cut and tubing connectors applied to form part A. An epoxy-molded IC is metalized and patterned with SU-8 channels to form part B. A and B are then joined using a clean room contact aligner (vacuum surfaces shown).

For this project, a new method was developed that avoided channel occlusion, creating a functional lid (Fig. 20). In this method, the lid is assembled separately first. The backing is removed from one side of a piece of PSA (9474LE 300LSE; 3M,

Maplewood, MN) and replaced with a piece of optically clear mylar. Here, the mylar was cleaned with isopropyl alcohol and dried prior to application to ensure strong adhesion and to prevent stray particles from begin trapped in the device. This assembly is laser-cut to create holes at the channel outlets and inlets as well as windows to access the connection pads made in the metallization step. Press fit tubing connectors are then added to the mylar side at channel inlets and outlets. A cleanroom contact aligner (MJB 3; Karl Suss (now SÜSS MicroTec), Garching, Germany) is used to place the lid on the SU-8 channel. The epoxy coupon is placed on the stage. The remaining backing is then removed from the lid. The lid is placed on the mask holder with the adhesive side down and vacuum sealed in place. The mask holder and stage are both slid under the microscope but kept in separation. As in photolithography, the two pieces are aligned under the microscope. Once aligned, the lid and coupon are brought into contact to evenly seal the lid to the coupon.

It is best to make the lid as large as possible (while still being able to clear the grooves of the contact aligner when sliding in) so that the lid extends well beyond the vacuum ring. If the lid edge is too near the ring, the lid may deform when the vacuum is applied and stick when sliding into the contact aligner or adhere to the substrate prematurely. Additionally, the stage may need to be manually raised after bringing the pieces into contact to ensure there is sufficient pressure to seal the channels. It is of note that the laser cut method described above also produces a functional and optically-clear lid, though at the cost of lower resolution channels. As single-cell-scale channels are needed for this application, the laser cut method would be insufficient.

4.5 Completed Device

A completed device was successfully created with the above method featuring metal integration, SU-8 channel integration, and microfluidic lid addition. A close up of the IC is pictured in Fig. 21, showing metal connections routing away from the IC as well as a fluid channel with and without fluid. A dye solution was injected through the tubing connectors on the top of the device via syringe, and inspection under a microscope (Fig. 21) shows the fluidic interface is leak-free. It is of particular note that no leaking is present at the boundary of the IC and epoxy. The boundary is the least planar region on the coupon as the epoxy molding process can result in slight beveling here. Success at this boundary is indicative of the robustness of the fluidic integration method.

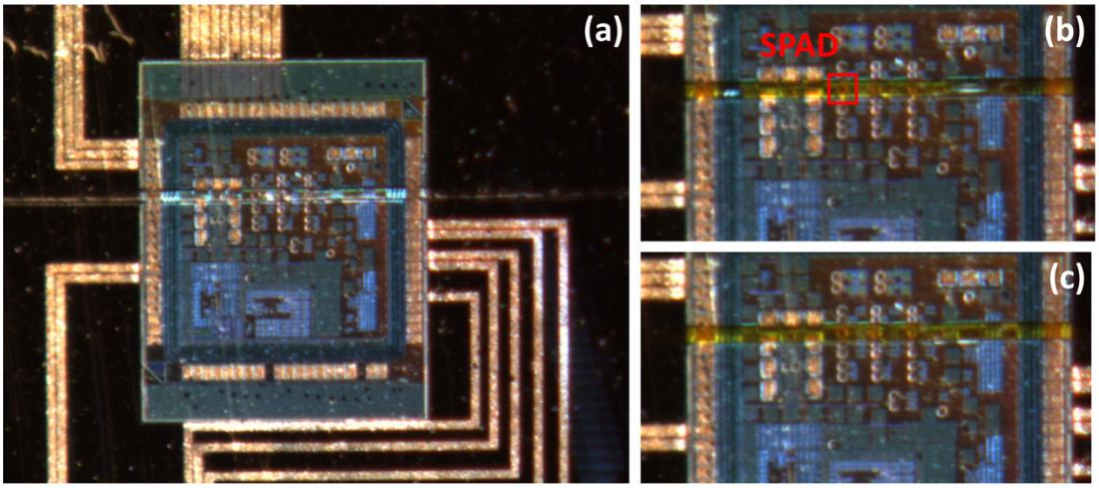

Fig. 21 Close-up view of a completed microfluidic device created using them metallization, SU-8, and lid method described above. (a) Full IC showing planar metal connections and unfilled fluid channel. (b) Partially-filled (containing dye solution and two air bubbles) fluidic channel over SPAD. (c) Fluidic channel over SPAD fully filled with dye solution.

5. Conclusion

This work describes two methods of microfluidic channel fabrication that can be integrated directly with CMOS integrated circuits. The first is a laser-cut fabrication method for rapid prototyping of channels using standard ‘maker’ tools, and the second is an SU-8 based approach for manufacturing higher resolution channel patterns. Both methods produce fully sealed channels and can be implemented directly over a metallized, epoxy-molded IC.

This is step towards creation of a CMOS-based cell counter, though the methods described could be leveraged to produce a variety of different devices integrating CMOS sensors and microfluidic channels. The next step in creating a CMOS-based cell counter specifically is to connect the device to a microcontroller to drive the SPAD and read light intensity data and test the sensor by running dyed fluids of different opacities through the channel. More opaque fluids should transmit less light and result in a drop in light intensity. Following this, the device would be characterized using ceramic beads as an analog for real cells, and subsequently used to measure the concentration of real cells suspended in solution. Further work could explore fluorescent labeling of cells to differentiate between cell types; this may involve multiple detectors in the same channel with different optical filters such that each is sensitive to a specific wavelength of light. The results shown here are promising and are expected to lead to more fully-integrated microfluidic/CMOS sensors in the future.

Works Cited

[1] S. Sengupta, H. Ouh, and M. L. Johnston, "An all-digital CMOS ambient light sensor using a single photon avalanche diode," in *2017 IEEE SENSORS*, 2017, pp. 1–3.

[2] M. Lindsay *et al.*, "Scalable Hybrid Integration of CMOS Circuits and Fluidic Networks for Biosensor Applications," presented at the IEEE Biomedical Circuits and Systems, p. 4.

[3] T. Beer, "Additional Thesis Discussion," 11-May-2018.

[4] Yu-Jie Huang *et al.*, "A CMOS Cantilever-Based Label-Free DNA SoC With Improved Sensitivity for Hepatitis B Virus Detection," *IEEE Trans. Biomed. Circuits Syst.*, vol. 7, no. 6, pp. 820–831, Dec. 2013.

[5] A. Manickam, A. Chevalier, M. McDermott, A. D. Ellington, and A. Hassibi, "A CMOS Electrochemical Impedance Spectroscopy (EIS) Biosensor Array," *IEEE Trans. Biomed. Circuits Syst.*, vol. 4, no. 6, pp. 379–390, Dec. 2010.

[6] J. M. Rothberg *et al.*, "An integrated semiconductor device enabling non-optical genome sequencing," *Nature*, vol. 475, no. 7356, pp. 348–352, Jul. 2011.

[7] J. Friend and L. Yeo, "Fabrication of microfluidic devices using polydimethylsiloxane," *Biomicrofluidics*, vol. 4, no. 2, Mar. 2010.

[8] M. Muluneh and D. Issadore, "A multi-scale PDMS fabrication strategy to bridge the size mismatch between integrated circuits and microfluidics," *Lab Chip*, vol. 14, no. 23, pp. 4552–4558, 2014.

[9] D. Welch and J. B. Christen, "Seamless integration of CMOS and microfluidics using flip chip bonding," *J. Micromechanics Microengineering*, vol. 23, no. 3, p. 035009, Mar. 2013.

[10] S. Chiavaroli, D. Newport, and B. Woulfe, "An optical counting technique with vertical hydrodynamic focusing for biological cells," *Biomicrofluidics*, vol. 4, no. 2, p. 024110, Jun. 2010.

[11] C.-T. Chiang, "Design of CMOS Monolithic Digitized Light Transducer With Calibration Technique for Ambient Light Sensor Applications," *IEEE Sens. J.*, vol. 13, no. 5, pp. 1931–1940, May 2013.

[12] X. Han, C. van Berkel, J. Gwyer, L. Capretto, and H. Morgan, "Microfluidic Lysis of Human Blood for Leukocyte Analysis Using Single Cell Impedance Cytometry," *Anal. Chem.*, vol. 84, no. 2, pp. 1070–1075, Jan. 2012.

[13] N. Haandbæk, O. With, S. C. Bürgel, F. Heer, and A. Hierlemann, "Resonance-enhanced microfluidic impedance cytometer for detection of single bacteria," *Lab. Chip*, vol. 14, no. 17, p. 3313, Jun. 2014.

[14] E. P. Dupont *et al.*, "Fluorescent magnetic bead and cell differentiation/counting using a CMOS SPAD matrix," *Sens. Actuators B Chem.*, vol. 174, pp. 609–615, Nov. 2012.

[15] Y. Chen *et al.*, "Portable Coulter counter with vertical through-holes for high-throughput applications," *Sens. Actuators B Chem.*, vol. 213, pp. 375–381, Jul. 2015.

[16] A. F. Coskun, T.-W. Su, and A. Ozcan, "Wide field-of-view lens-free fluorescent imaging on a chip," *Lab. Chip*, vol. 10, no. 7, p. 824, 2010.

[17] M. Lindsay *et al.*, "Heterogeneous Integration of CMOS Sensors and Fluidic Networks using Wafer-Level Molding," *IEEE Trans. Biomed. Circuits Syst.*, To Appear.